Noncontact surface temperature measurement by means of a modulated photothermal effect

Thierry Loarer, Jean-Jacques Greffet, Magdeleine Huetz-Aubert

Noncontact surface temperature measurement by means of a modulated photothermal effect

Thierry Loarer, Jean-Jacques Greffet, and Magdeleine Huetz-Aubert

The main problems when measuring surface temperature by means of radiometry (i.e., optical pyrometry) are the unknown emissivity and radiation reflected by the sample. The latter problem becomes critical when the sample is placed in hot surroundings, such as furnaces or combustion chambers; indeed, the reflected flux may then become larger than the emitted flux. In this paper we describe a novel technique, based on the photothermal effect, which allows the surface temperature to be measured without error due to reflected fluxes. The influence of the parameters of the experimental setup are discussed. Experimental data obtained with a sample placed inside a furnace are reported in the (300–1150 K) range. The experimental results show the efficiency of the technique which proves to be a general solution to extend the domain of application of optical pyrometry.

I. Introduction

Optical pyrometry is a well known technique for measuring surface temperature. It is based on the detection of the flux emitted by the target, generally in the IR part of the spectrum. In classical optical pyrometry, the best results are obtained when the emissivity is nearly equal to unity and when the surface temperature is much higher than the ambient. When trying to deduce the temperature from the measured signal, three problems arise:

(i) The first problem is well known. The value of the emissivity varies widely for different materials and is generally unknown. Dependence of emissivity values on temperature, angle, polarization, and wavelength are studied in published data.[1–3] In industrial applications, the emissivity values also depend on roughness, contamination, and oxidation; therefore, these values have to be used with care. The reader will find in a review by Nutter[4] the description of some techniques that compensate for unknown variation in emissivity.

Another method, multiwavelength pyrometry, has been developed to obviate the need to know surface emissivity. A polynomial expression of the emissivity as a function of wavelength allows the determination of surface temperature.[5–8] The most simple is the so-called two-color technique which allows the surface temperature to be calculated from the ratio of spectral fluxes measured for two separate wavelengths. Then, the ratio of emissivities can be either assumed equal to one[9] or to a previously measured value.[10]

(ii) The second problem, namely reflected fluxes, becomes important when measuring the temperature of surfaces placed in hot surroundings; for instance, a furnace or a combustion chamber. The same problem is encountered when measuring the surface temperature of samples with high reflectance. Until recently, no general solution existed for this second problem. A possible solution consists of estimating the value of the reflected fluxes by auxiliary measurements, and then using this value in a radiative transfer model. For instance, gas turbine blade temperature measurements require complex computer models[11] which take into account the radiative transfer between the blades and the surroundings. In this method, pyrometers collect emitted flux from the front face and the back face of the blade. Knowing emissivity, the computer model allows surface blade temperature to be determined.

In furnaces, the geometry is generally less complex. Several methods allow the reflected flux to be estimated. Dual-pyrometer reflectivity compensation methods for the determination of metal temperature are given by Roney.[12] In this approach, an auxiliary pyrometer receives a signal caused solely by the reflected component from the furnace interior. This method allows the signal provided by the sample to be corrected to obtain the surface temperature. Instead of measuring the reflected radiance, the shielded target

The authors are with Centre National de la Recherche Scientifique et Ecole Centrale Paris, Laboratoire d'Energétique Moléculaire et Macroscopique, Combustion, 92295 Châtenay-Malabry CEDEX, France.

method[13] is often used when inspecting diffuse surfaces. However, this method requires complicated setups which are not always conveniently installed in industrial applications. Another method consists of covering the heated surface with a highly reflective hemisphere, under the assumption that no perturbation is induced on surface temperature.[4] The multiple reflections increase the flux; thus the effective emissivity of the target is expected to be almost one.[14] Similar methods use two cavities, one reflecting and one absorbing. From measurements taken from the two cavities, both emissivity and temperature can be deduced.[15]

(iii) The third problem is due to the absorption by the gases between the surface and the detector. This problem will be discussed in Sec. IV.

From this rapid overview, it appears that the two main problems are the unknown emissivity and the reflected fluxes and that no general solution allows these problems to be solved.

In this paper, we present a technique which allows the surface temperature to be measured without the introduction of error due to the reflected fluxes. The basic idea consists of creating a local, weak, and time dependent modification of the sample surface temperature. For this purpose, we focus a chopped laser beam on the surface of the sample. Thus, the emitted flux has a dynamic component whereas the reflected flux remains constant. Therefore, the dynamic component of the signal is only due to the emitted flux and depends only on emissivity and sample surface temperature, designated as T_0. Throughout this paper, we consider modulated heating. On the other hand, pulsed heating is also possible and allows very rapid temperature measurements on moving samples to be made. Work on this alternative is in progress.[16]

In Sec. II, theoretical considerations related to temperature fields and measured photothermal signals are presented. In Sec. III we present a method which enables us to deduce surface temperature. The experimental setup is described in Sec. IV. Experimental results and an extension of this method to low temperatures, useful for monitoring applications, are described in Sec. V.

II. Theoretical Considerations

The flux leaving a solid surface of an opaque material at temperature T_0 in a surrounding assumed to be a blackbody at temperature T_a in a specified direction, is described by its radiance L_λ^e, and can be written in the form

$$L_\lambda^e = \epsilon_\lambda' L_\lambda^\circ(T_0) + (1 - \epsilon_\lambda')L_\lambda^\circ(T_a), \tag{1}$$

where L_λ° stands for the blackbody radiance and ϵ_λ' for the spectral directional emissivity.

Only the first term on the right hand side, the emitted radiance, depends on the sample surface temperature; however, a detector cannot separate the reflected flux from the emitted flux. Classical optical pyrometry assumes that reflected fluxes are negligible. Figure 1 shows values of measured temperatures T_m with a

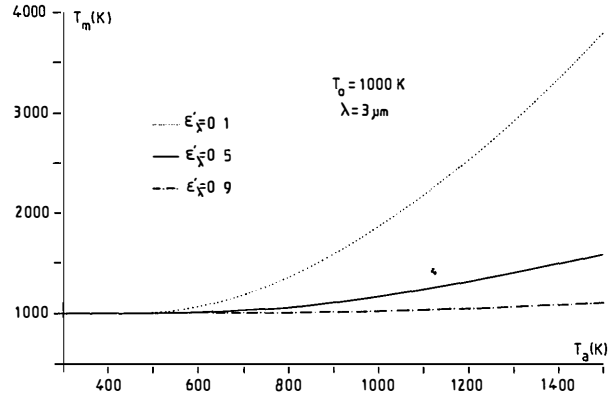

Fig. 1. Influence of the reflected fluxes on the measured temperature T_m by classical optical pyrometry given by $L_\lambda^e = \epsilon_\lambda' L_\lambda^\circ(T_m)$. The sample at $T_0 = 1000$ K is placed in a surrounding at temperature T_a and three monochromatic emissivities of the sample are considered: ----- $\epsilon_\lambda' = 0.1$, —— $\epsilon_\lambda' = 0.5$, —·— $\epsilon_\lambda' = 0.9$.

monochromatic pyrometer given by $L_\lambda^e = \epsilon_\lambda' L_\lambda^\circ(T_m)$ assuming that the spectral directional emissivity is known. It appears that optical pyrometry cannot be used when $(1 - \epsilon_\lambda')L_\lambda^\circ(T_a) > \epsilon_\lambda' L_\lambda^\circ(T_0)$, which may occur for low values of the emissivity or high values of the ambient temperature T_a. It is the purpose of this paper to give a general solution to this problem.

The principle of the method is based on the photothermal effect[17,18] and has been previously reported.[19–21] A chopped laser beam is focused on the target; thus a local and time dependent modification of the temperature is generated and denoted as $\Delta T(t)$. Assuming that $\Delta T(t) \ll T_0$, the expression for the total radiance (emitted and reflected) radiance can be written in the form

$$L_\lambda^e(T_0) = \epsilon_\lambda' L_\lambda^\circ(T_0) + (1 - \epsilon_\lambda')L_\lambda^\circ(T_a) + \epsilon_\lambda' \frac{\partial L_\lambda^\circ}{\partial T}(T_0)\Delta T(t) + \frac{\partial \epsilon_\lambda'}{\partial T}[L_\lambda^\circ(T_0) - L_\lambda^\circ(T_a)]\Delta T(t). \tag{2}$$

For a solid, the variation of emissivity within a small temperature interval (<10 K) can be neglected.[18,21] Due to this fact, the last term of the right hand side of Eq. (2) can be discarded. More precisely, the condition to be fulfilled is

$$\frac{1}{\epsilon_\lambda'}\frac{\partial \epsilon_\lambda'}{\partial T} \ll \frac{1}{[L_\lambda^\circ(T_0) - L_\lambda^\circ(T_a)]}\frac{\partial L_\lambda^\circ}{\partial T}. \tag{3}$$

The radiation leaving the solid surface appears to be the sum of a continuous term and a dynamic term. The continuous term contains the reflected and emitted radiation and the dynamic term only depends on time, surface temperature, and emissivity. Therefore, by filtering the electrical signal delivered by the infrared detector, it is possible to separate the reflected flux from the emitted flux.

We can use either pulsed or modulated temperature variation. In the discussion which follows, we only consider modulated excitation. Let us calculate the temperature field due to a laser beam modulated at a frequency f travelling in the z-direction and heating

the sample surface initially at temperature T_0. Assuming that the laser beam intensity has a Gaussian profile, the Rosencwaig-Gersho theory[22] permits the precise calculation of the induced temperature distribution $\Delta T(r,t)$, where r is the distance from the center of the Gaussian spot and t is the time. The temperature field can be written as

$$\Delta T_0(r) + \sum_n \Delta T_n(r,f_n) \exp(2\pi j f_n t), \tag{4}$$

where $\Delta T_0(r)$ is the stationary field and $f_n = nf$.

By using a lock-in amplifier, only the first order harmonic will be detected. Then, the temperature of the surface is given by

$$T(r,t) = T_0 + \Delta T_0(r) + \Delta T_1(r) \exp(2\pi j f t). \tag{5}$$

Detailed expressions for temperature fields are given in Appendix A. In particular, it is shown that ΔT_0 and ΔT_1 are proportional to the absorbed power P. For convenience, we will omit the r and t temperature field dependence hereafter. In Appendix B, we derive the main features of ΔT_1 in a simple way.

The spectral radiance due to emission can be expanded to first order and can be written in the form

$$\epsilon'_\lambda L^\circ_\lambda(T_0 + \Delta T_0 + \Delta T_1) = \epsilon'_\lambda L^\circ_\lambda(T_0 + \Delta T_0) + \epsilon'_\lambda \left\{ \frac{\partial L^\circ_\lambda}{\partial T}(T_0)\Delta T_1 + \frac{\partial^2 L^\circ_\lambda}{\partial T^2}(T_0)\Delta T_1 \Delta T_0 \right\} \times \exp(2\pi j f t). \tag{6}$$

The dynamic term is the second on the right hand side of Eq. (6). The detected signal is proportional to the dynamic radiative flux integrated over the spectral bandwidth $\Delta\lambda$ of the interference filter. We assume that $\Delta\lambda$ is small enough to allow the variations of the other terms to be neglected. In Sec. III, we discuss how it is possible to account for the variation of $\partial L^\circ_\lambda/\partial T$ when the bandwidth is increased. Within this approximation, and considering an area ΔS of the viewed surface with a solid angle of viewing $\Delta\Omega$, the spectral signal S_λ delivered by an IR detector is proportional to the dynamic term and is given by

$$S_{\lambda_p} = \tau_{\lambda_p} D_{\lambda_p} \epsilon'_{\lambda_p} \Delta\lambda \Delta\Omega \times \left(\frac{\partial L^\circ_{\lambda_p}}{\partial T}(T_0) \int_{\Delta S} \Delta T_1 dS + \frac{\partial^2 L^\circ_{\lambda_p}}{\partial T^2}(T_0) \int_{\Delta S} \Delta T_0 \Delta T_1 dS \right), \tag{7}$$

where D_{λ_p} is the responsivity of the detector, and $\tau_{\lambda p}$ is the peak value of the spectral transmittance τ_λ of the optical system in the spectral window $\Delta\lambda$ (FWHM) defined by

$$\int_0^\infty \tau_\lambda d\lambda = \tau_{\lambda_p} \Delta\lambda. \tag{8}$$

For convenience, we will omit the p-index hereafter.

Figure 2 shows an experimental example of the photothermal signal S_λ as a function of laser power P_0. The nonlinear behavior, due to the second term on the right hand side of Eq. (7), appears at higher power levels, whereas at low power the signal is linear with respect to P_0. In addition, it appears that the signal is proportional to $[\partial L^\circ_\lambda/\partial T](T_0)$ in the linear zone, whereas the signal delivered by a classical pyrometer is proportional to $L'_\lambda(T_0)$.

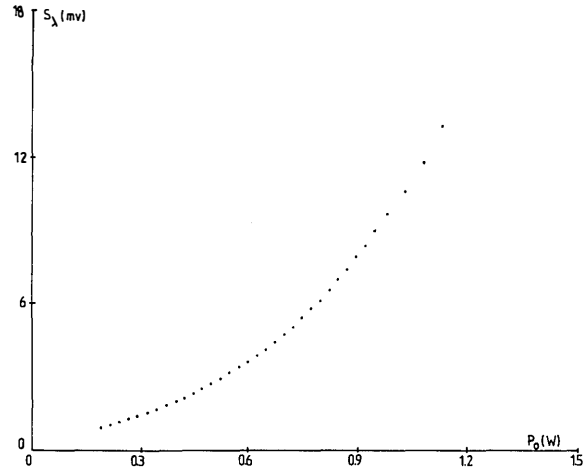

Fig. 2. Photothermal signal S_λ vs laser power P_0 for a 304L steel sample, with the following experimental parameters: $T_0 = 700$ K, $f = 35$ Hz, $\lambda = 3.99$ μm, $\Delta\lambda = 160$ nm, $\epsilon'_\lambda = 0.85$.

III. Temperature Measurement

A. Temperature Measurement from the Photothermal Signal

In the case of low laser power, the photothermal signal S_λ delivered by the detector and the lock-in amplifier [see Eq. (7)], depends on three unknown parameters: the surface temperature, the emissivity, and the dynamic component of the surface temperature ΔT_1 induced by the laser beam. An expression for the latter can be deduced from theoretical considerations (see Appendix A) in terms of the laser power and the thermophysical properties of the studied material. In practice ΔT_1 cannot be determined with sufficient accuracy; thus we have to eliminate this quantity.

For this purpose we will consider, according to Eq. (7) and Eq. (8), only the region where the signal is proportional to the absorbed power at low level (see Fig. 2). More specifically, the signal can be written in the form

$$S_\lambda = D_\lambda \epsilon'_\lambda \Delta\Omega \tau_\lambda \Delta\lambda \frac{\partial L^\circ_\lambda}{\partial T}(T_0) \int_{\Delta S} \Delta T_1 dS, \tag{9}$$

where ΔS is the irradiated area. It is important to point out that the signal comes exclusively from this irradiated region; therefore the spatial resolution of the measurement is controlled with great accuracy. This feature could be of great interest in measuring surface temperatures of solid state devices for instance.

To eliminate ΔT_1, we perform two measurements at two different wavelengths, λ_1 and λ_2, and we take the ratio of the two signals obtained. This procedure also allows all the geometrical terms of Eq. (9) to be eliminated. The ratio depends no longer on the dynamic surface temperature, but does depend on the values of

emissivity at λ_1 and λ_2. For many cases, the Wien's function will provide a very good approximation. The surface temperature can then be written in closed-form as

$$T_0 = \frac{C_2\left(\frac{1}{\lambda_2} - \frac{1}{\lambda_1}\right)}{\ln\left\{\frac{S_{\lambda_1}}{S_{\lambda_2}}\frac{\epsilon'_{\lambda_2}}{\epsilon'_{\lambda_1}}\frac{\tau_{\lambda_2}D_{\lambda_2}\Delta\lambda_2}{\tau_{\lambda_1}D_{\lambda_1}\Delta\lambda_1}\left(\frac{\lambda_1}{\lambda_2}\right)^6\right\}}, \quad (10)$$

where C_2 is the second radiation constant ($C_2 = 14388$ μmK).

In practice, it is possible to increase the accuracy of the measurements by working at several different powers within the linear region. The slope S_λ/P_0 can then be measured with great accuracy, so we use the ratio of the slopes instead of the ratio of the signals. However, the measurements at a single value of the power generally provide faster and sufficiently accurate measurements.

B. How to Eliminate the Emissivity

At this stage, we have to eliminate the unknown ratio $\epsilon'_{\lambda_1}/\epsilon'_{\lambda_2}$ appearing in Eq. (10). It must be pointed out that we now meet the classical problem of the unknown emissivity. To proceed, we can either measure this ratio[10] or use the so-called two-color technique. In this paper, we focus our attention on the problem of errors due to the reflected radiations. Therefore, we adopt the simpler solution, i.e., the two-color technique, assuming $\epsilon'_{\lambda_1} = \epsilon'_{\lambda_2}$ in Eq. (10). In Sec. V we present results obtained by means of this technique.

In what follows, we present an alternate technique that may be used to deduce temperature from the measured signal without making any assumption about the emissivity. However, we will not present experimental data obtained by this technique for reasons that will appear later. Note that until now, we have not used all the information provided by the photothermal signal. Considering again Eq. (7), the second term of the right hand side is proportional to ΔT_0 and ΔT_1. Because both ΔT_0 and ΔT_1 are proportional to the laser power P_0, it turns out that the photothermal signal has a quadratic dependence on P_0 and can be written in the form

$$S_\lambda = a_\lambda P_0 + b_\lambda P_0^2. \quad (11)$$

The behavior is observed experimentally (Fig. 2). It is possible to obtain the parabolic coefficients a_λ and b_λ by a curve fit. The main point is that the emissivity can be eliminated without any approximation by taking the ratio of these coefficients. The resulting form follows

$$\gamma_\lambda = \frac{b_\lambda}{a_\lambda} = c\frac{\frac{\partial^2 L^\circ_\lambda}{\partial T^2}(T_0)}{\frac{\partial L^\circ_\lambda}{\partial T}(T_0)}, \quad (12)$$

where c is the ratio of the integrals appearing in Eq. (7). The ratio γ_λ is a function of the temperature and does not depend on emissivity at λ_1 and λ_2. To deduce the temperature from this ratio, we have to know the value of the constant c. For a given material this quantity can be calibrated. For the more general case, it can be eliminated by taking the ratio of two values of γ_λ for two different wavelengths. This ratio can be written in the form:

$$\frac{\gamma_{\lambda_1}}{\gamma_{\lambda_2}} = \frac{[\exp(A_1) - 1]\{2A_2\exp(A_2) - (2 + A_2)[\exp(A_2) - 1]\}}{[\exp(A_2) - 1]\{2A_1\exp(A_1) - (2 + A_1)[\exp(A_1) - 1]\}} \quad (13)$$

where $A_1 = C_2/(\lambda_1 T_0)$ and $A_2 = C_2/(\lambda_2 T_0)$.

Unfortunately, this technique has some drawbacks. Equation (13) is not sufficiently sensitive with respect to temperature unless one use very different wavelengths. It turns out that we cannot expect to have good signal to noise ratios for both wavelengths if they are very different unless the temperature is high. In addition, the result relies highly on the accuracy of the parabolic coefficients a_λ and b_λ—this is certainly the major limit of the approach.[21] Some attempts have been made with this technique; we have been able to obtain the parabolic coefficients with an accuracy better than 1% for the linear term and only 5% for the quadratic term. Since we used an IR detector, we have chosen the two wavelengths in order to have a good detectivity (between 2 and 5 μm). With such wavelengths, the ratio appearing in Eq. (13) has a weak dependence on T; therefore the error on te measurement leads to a large error for the temperature. However, by using a visible detector (photomultiplier) and an infrared detector, this method should be a valuable tool to eliminate the emissivity.

C. Domain of Application of the Method

The technique will be limited by the capability of measuring the detected signal. It appears clearly in Eq. (7) that the signal is proportional to the product $\Delta S\Delta\Omega$, the bandwidth $\Delta\lambda$ of the filter, the absorbed power, and the responsivity of the detector D_λ. These factors are fixed by the designer of the experimental setup. On the other hand, there are two parameters which affect the signal and are dependent on the target. These two parameters are the emissivity ϵ'_λ and the first derivative of the Planck's function with respect to temperature. The minimum signal that can be detected is given by the noise equivalent power (NEP) of the detector, defined as a flux providing a signal-to-noise ratio equal to one. Thus for a given experimental setup, this limit caused by the detector will lead to a minimum value of the product of the emissivity and the first derivative of the Planck's function with respect to temperature:

$$\Delta\Omega\Delta\lambda\tau_\lambda\Delta S\frac{\Delta T_{1\max}}{2}\epsilon'_\lambda\frac{\partial^\circ_\lambda}{\partial T}(T_0,\lambda) \geq 10\ \text{NEP}. \quad (14)$$

In Eq. (14) $\Delta T_{1\max}\Delta S/2$ stands for an approximate value of the integral over the heated region

$$\int_{\Delta S}\Delta T_1 dS \approx \frac{\Delta T_{1\max}}{2}\Delta S. \quad (15)$$

Knowing the experimental setup, this relation allows the emissivity and temperature range to be determined. The choice of the bandwidth of the interfer-

ence filters and their peak value positions will be considered in the next section.

D. Wavelength Determination

We now turn to the problem of choosing the wavelengths. It can be shown that the sensitivity of the signal as a function of temperature increases when the difference $\lambda_2 - \lambda_1$ is increased. In order to illustrate this feature, we have displayed in Fig. 3 a set of curves $\partial L^\circ_\lambda/\partial T$ vs λ for different values of T_0. Recall that our measurement is proportional to $(\partial L^\circ_{\lambda_1}/\partial T)/(\partial L^\circ_{\lambda_2}/\partial T)$. It turns out from Fig. 3 that this ratio will be almost constant if λ_1 and λ_2 are very close. This will result in a very weak dependance of the measured quantity on the temperature.

Since $(\partial L^\circ_\lambda/\partial T)$ is an increasing function of T_0 for any λ, it turns out that highest sensitivity is achieved by choosing one wavelength with a very high or very low value (where the dependance on T_0 is very weak) and the other in the region where the dependance on T_0 is maximum. Within the assumption that $\partial L^\circ_{\lambda_2}/\partial T(T_0)$ is almost constant, the signal varies as $\partial L^\circ_{\lambda_1}/\partial T(T_0)$; the sensitivity as $\partial^2 L^\circ_\lambda/\partial T^2$, and its maximum is given by

$$\frac{\partial}{\partial\lambda}\left(\frac{\partial^2 L^\circ_\lambda}{\partial T^2}(T_0)\right) = 0. \tag{16}$$

This condition leads to the relation

$$\lambda T_0 = 1957\ \mu\text{m-K}. \tag{17}$$

A second condition is due to signal level. Obviously, the accuracy of the measurement requires a good signal-to-noise ratio. Thus one has to work with a wavelength chosen in the vinicity of the maximum of the first derivative of the Planck's function with respect to T_0 (i.e. $\lambda T_0 = 2410\ \mu$m-K[18]).

Finally, one might think that choosing both wavelengths close to one another would reduce the error due to the graybody assumption. As a matter of fact, within the Wien approximation, the relative error can be written in the form

$$\frac{1}{T_m} - \frac{1}{T_0} = \frac{\ln\left(\dfrac{\epsilon'_{\lambda_2}}{\epsilon'_{\lambda_1}}\right)}{C_2\left(\dfrac{1}{\lambda_1} - \dfrac{1}{\lambda_2}\right)}, \tag{18}$$

where T_0 is the true temperature and T_m the measured temperature assuming $\epsilon_{\lambda_1} = \epsilon_{\lambda_2}$. From this equation, it is seen that the relative error is not necessarily reduced by choosing wavelengths very close to each other since the denominator will be decreased. If the emissivity has a small slope with respect to λ, the logarithm of the ratio of emissivities will vary slower than the difference $\lambda_2 - \lambda_1$ appearing in the denominator. Therefore, if one knows that the emissivity has a slow variation rate, as it is the case for oxidized steel, it is convenient to have a large difference $\lambda_2 - \lambda_1$.

A final requirement must be taken into account, namely, the absorption bands of the air in the IR spectrum. The transmission wavelengths of the interference filters must be chosen outside the absorption

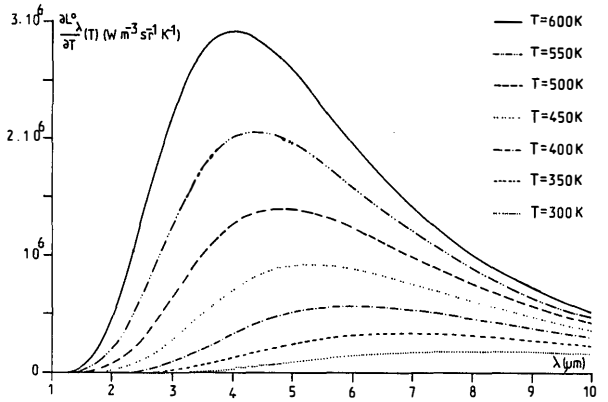

Fig. 3. First derivative of Planck's function with respect to temperature vs wavelength.

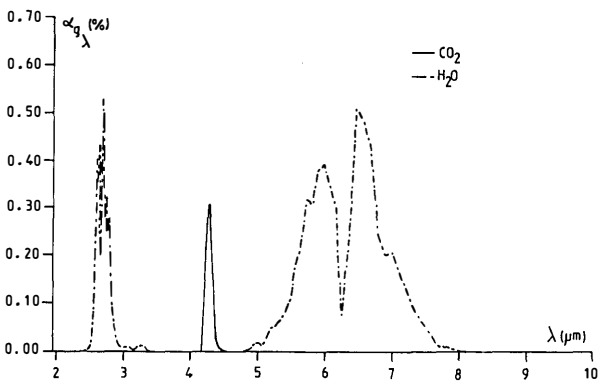

Fig. 4. Absorption factor $\alpha_{g\lambda}$ of a mixture at 300 K of N_2(96.867%), H_2O(3.1%) and CO_2(0.033%) vs the wavelength λ in a 50-cm cell.[25]

bands of H_2O and CO_2.[23–25] Figure 4[25] shows the average absorption factor $\alpha_{g\lambda}$ of a mixture of N_2 (96.867%), H_2O (3.1%) and CO_2 (0.033%) at 300 K vs the wavelength λ, in a 50-cm cell. It can be seen that the absorption in the 5.5–8-μm and 2.5–3-μm ranges is very intense. Since the concentration of H_2O may vary, the signal is subject to large variations. For instance, in the range between 300–400 K, we cannot use the best wavelength defined by Eq. (17). The absorption due to CO_2 is also very intense at 4.26 μm.

IV. Experimental Setup

The experiment consists of measuring the surface temperature of a sample placed inside a furnace. With this configuration, the reflected flux is clearly very large and so serves as an excellent test of our technique. Figure 5 shows the experimental details. The laser beam used to create the photothermal effect is modulated by a mechanical chopper. The laser beam wavelength must be out of the spectral detection bandwidth. It is also convenient to choose this wavelength taking into account the absorptivity of the sample. An Argon laser beam with an emission wavelength of $\lambda_0 = 514.5$ nm is used.

The sample is a 304L steel cylinder, which is 6-mm thick and 60 mm in diameter. Its temperature is regu-

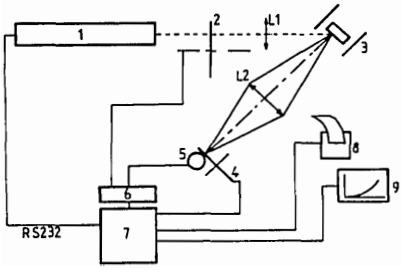

Fig. 5. Experimental setup: 1, argon laser; 2, mechanical chopper; 3, furnace and sample; 4, interference filter; 5, infrared detector (InSb); 6, lock-in amplifier; 7, Apple II micro-computer; 8, printer; 9, plotter; L_1, glass lens; L_2, CaF_2 lens.

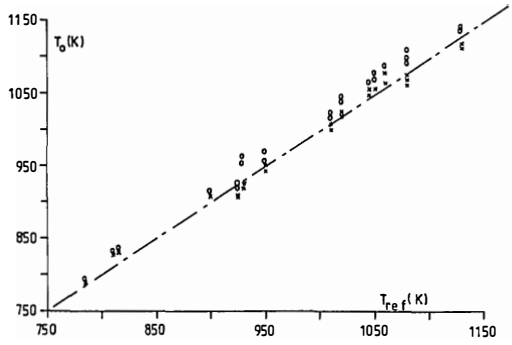

Fig. 6. Measured temperature T_0 vs reference temperature T_{ref} in the 750–1150 K range, for two pairs of wavelengths: x[1.7–1.97 μm], o[1.7–2.1 μm].

lated by using two thermocouples lying at 1 and 2 mm from the surface respectively. The accuracy of the thermocouples is better than 0.5%. It can be shown that the temperature difference between the sample and the thermocouples is negligible. A linear extrapolation gives the surface temperature with an estimated ±1% accuracy.

A glass lens L_1 focuses the beam to form a spot of between 1–2 mm in diameter on the sample surface. The optical detection path includes a CaF_2 lens L_2 which collects the exiting radiance and focuses it onto the detector through an interference filter. The IR detector is used at a single wavelength which we denote λ_1. The laser light at λ_0 reflected on the sample is modulated, so it may lead to a systematic error if the interference filter attenuation at λ_0 is insufficient. Thus a highpass filter has to be placed at the back of the interference filter. The same problem arises due to the IR radiance of the laser discharge. This IR flux is eliminated by the focusing glass lens L_1 which does not transmit above its cutoff wavelength λ_g. If $\lambda_1 < \lambda_g$, an additional lowpass filter placed behind L_1 has to be used.

Fine mechanical adjustments enable the detector surface to be conjugated with the sample surface. The spectral transfer functions of the optics, filters and detector have been calibrated by using a standard blackbody and a pyroelectric detector for which the spectral responsivity is constant. The IR detector is a liquid nitrogen cooled InSb (Infrared Associates). It delivers an electrical signal which is then fed into a lock-in amplifier (PAR 5204) working with a time constant of 1 s. Data acquisition, as well as the rotation of interference filters and the laser power are controlled by an AppleII computer.

V. Experimental Results

The two-color technique is most accurate for narrow bandwidths. However, the signal is reduced when the bandwidth becomes narrower. Thus the choice of the bandwidth is a function of the signal level.

A. Temperatures >750 K

From Eq. (17), it can be seen that in this range of temperature, we have to work with wavelengths centered near 2 μm; the pairs of wavelengths are 1.7–1.97 μm and 1.7–2.1 μm. The sample is heated by a radiative furnace, hence the surface furnace temperature must be ~1000 K to get a sample surface temperature of 750 K. The sample emissivity near 2 μm is 0.85, and using Eq. (1), it can be shown that the reflected flux is higher than the emitted flux. This difference increases with the surface furnace temperature.

For a value of emissivity >0.1, a filter with a bandwidth as narrow as 40 nm will provide a very good signal with the following experimental parameters: $\Delta\Omega\Delta S = 1.2 \times 10^{-8}$ m^2 sr, $\tau_\lambda = 0.5$, $\Delta T_{1\max} \approx 6$ K, $T_0 \geq 750$ K, $f = 35$ Hz, time constant = 1 s, and NEP = 10^{-10} W.

Figure 6 displays some typical experimental temperature measurements made on a 304L steel sample. The reference temperature T_{ref}, displayed on the x-axis, is obtained by using two thermocouples buried in the sample 1 mm and 2 mm under the interface. The surface temperature measurement T_0, obtained by means of a modulated photothermal effect, using the two pairs of wavelengths, is displayed on the y-axis. The discrepancies between T_{ref} and T_0 are <3%. There is a systematic difference between the measurement for the two pairs of wavelengths, and this error is due to the gray body assumption which is not perfectly satisfied near 2 μm. The reproducibility is better than 2%. Finally, although the reflected flux is larger than the emitted flux as stated above, no systematic error appears; this clearly shows that the reflected flux is completely eliminated.

B. Temperatures: 340–750 K

We define low temperatures as being in the range between 340–750 K. For low temperatures, larger values of the wavelengths need to be used. In the region 5.5–8 μm the absorption by laboratory air is important. In practice, we use two wavelengths at 3.99 μm and 4.74 μm with a 160-nm bandwidth. Since the temperature is lower, the signal is lower. In order to compensate for this decrease in signal strength, we can either use a more powerful laser or larger bandwidths. In the case of a more powerful laser, we have to increase the illuminated area in order to be sure that ΔT remains lower than ~10 K; thus the technique is nonintrusive and the first-order expansion of Eq. (6) is still valid. For larger

bandwidths, we must take into account the variation of the first derivative of the Planck's function with respect to temperature in the spectral bandwidth of the filter. Under the graybody assumption, the solution is given by the relationship

$$\frac{S_{\lambda_1}}{S_{\lambda_2}} = \frac{D_{\lambda_1}}{D_{\lambda_2}} \frac{\int_0^\infty Rf_1(\lambda) \frac{\partial L_\lambda^\circ}{\partial T}(\lambda, T_0) d\lambda}{\int_0^\infty Rf_2(\lambda) \frac{\partial L_\lambda^\circ}{\partial T}(\lambda, T) d\lambda}, \tag{19}$$

where $Rf_1(\lambda)$ and $Rf_2(\lambda)$ are respectively the spectral responses of the filters at the wavelengths $\lambda_1 = 3.99\ \mu m$ and $\lambda_2 = 4.74\ \mu m$.

Using Planck's law, a computer program has been written to solve numerically Eq. (19), assuming the response of the detector to be constant over the detection bandwidth. The transmittivities of the filters have been digitized; thus the integrals appearing in Eq. (19) can be numerically computed. Figure 7 displays the ratio of the integrals appearing in Eq. (19) as a function of the surface temperature in the 300–800 K range. This curve can be described as a function of $1/T_0$ whose coefficients are obtained by using the least-squares method. The maximum difference between the two curves is $<2 \times 10^{-4}$ when the equation is written as a second order polynomial. Eq. (19) can then be written in the form

$$\frac{S_{\lambda_1}}{S_{\lambda_2}} = 1.769 - \frac{720.6}{T_0} + \frac{85358}{T_0^2}. \tag{20}$$

From Eq. (20), the surface temperature can be easily deduced. The accuracy of the polynomial approximation can always be increased by including terms of higher order. The surface temperature is then determined by means of an iterative process.

The experimental data are displayed in Fig. 8 where the axes are defined as in Fig. 6. It can be seen that temperatures as low as 340 K can be measured and that no systematic error due to the reflected fluxes appears. The accuracy of the temperature measurements is ~3%, and as it has been outlined in the preceeding section, the limit of validity can be given as

$$\Delta\Omega\Delta\lambda\tau_\lambda\Delta S \frac{\Delta T_{1\max}}{2} \epsilon_\lambda' \frac{\partial L_\lambda^\circ}{\partial T}(T_0, \lambda) \geq 9 \times 10^{-10}\ \mathrm{W}, \tag{21}$$

where $\Delta\Omega\Delta S = 3 \times 10^{-8}\ \mathrm{m^2\ sr}$, $\tau_\lambda = 0.5$, $\Delta T_{1\max} \approx 6$ K, $\Delta\lambda = 160$ nm, $\epsilon_\lambda' = 0.85$, $\lambda = 4.744\ \mu m$, $T_0 = 340$ K, $f = 35$ Hz, time constant = 1 s, time averaging ≥ 3 s, and N.E.P. = 10^{-10} W.

For example, for the same conditions and with a black sample, the minimum temperature would be 332 K.

Note that the process defined by Eqs. (19) and (20) resembles the introduction of effective[26,27] and reference[28–31] wavelengths.

C. Temperatures: 260–340 K

In this section, we consider low temperatures (or highly reflecting surfaces). If the level of the signal does not allow the two-color technique to be used, we must change to a broadband filter. This means that

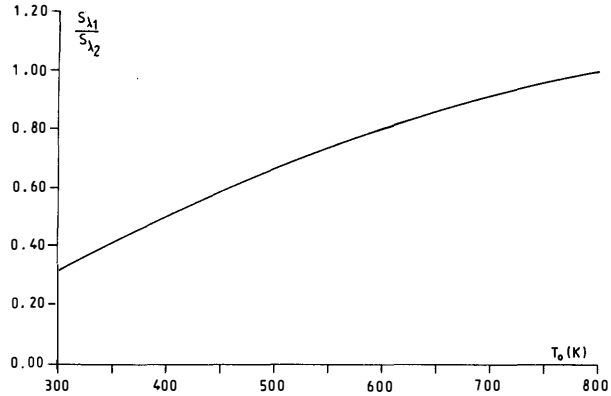

Fig. 7. Signal ratio vs surface temperature T_0, for the pair of interference filter wavelengths $\lambda_1 = 3.99\ \mu m$ and $\lambda_2 = 4.74\ \mu m$.

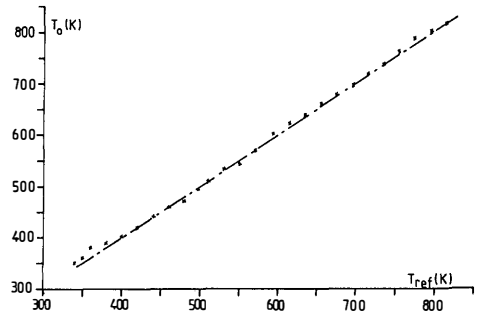

Fig. 8. Measured temperature $T_0(x)$ vs the reference temperature T_{ref} (——) in the 300–750 K range, for the pair of wavelengths: 3.99–4.74 μm.

we cannot deduce the temperature from the signal which results from the photothermal measurement. However, the signal is still an increasing function of temperature. Thus, if we calibrate the signal, we can obtain a very accurate technique to measure the temperature. Moreover, since the dependence of the signal on the temperature is given by the first derivative of the Planck's function, a single point is sufficient to calibrate the entire signal vs temperature curve. Since no ratio is required to eliminate the temperature variation, we do not have to work in the region where the signal is proportional to the incident power, so it can be increased. The photothermal signal can be written in the form

$$S_\lambda = \Delta\Omega \int_{\lambda_d}^{\lambda_h} \epsilon_\lambda' \tau_\lambda D_\lambda \left(\int_{\Delta S} \frac{\partial L_\lambda^\circ}{\partial T}(T_0) \Delta T_1 dS + \int_{\Delta S} \frac{\partial^2 L_\lambda^\circ}{\partial T^2}(T_0) \Delta T_1 \Delta T_0 dS \right) d\lambda, \tag{22}$$

where λ_d and λ_h are the low and high limits respectively of the broadband transmission filter. The bandwidth of the filter is 2.2 μm defined between $\lambda_d = 3.3\ \mu m$ and $\lambda_h = 5.5\ \mu m$.

Using this technique, we have been able to measure temperatures as low as 300 K on stainless steel samples with an emissivity as low as 0.4 (see Fig. 9). The laser power P_0 was 2 W, the beam spot (0.7 mm) was large enough to avoid high dynamic temperature compo-

nents, and the frequency was 35 Hz. The collecting lens was placed at 400 mm from the sample and its diameter was 36 mm. Since the signal-to-noise ratio was still very good, an approximation similar to Eq. (21) was used to estimate that accurate measurements could be performed at temperatures as low as 260 K with this experimental setup and a black sample.

It is clear that the technique can be used for industrial inspection in a variety of situations, such as the nonintrusive monitoring of temperatures of highly reflecting surfaces, or for monitoring temperatures of surfaces placed in hot environments like combustion chambers, furnaces, etc.

VI. Conclusion

We have presented a technique which greatly improves the domain in which optical pyrometry can be used. It has been shown that this technique allows the emitted flux to be rigorously separated from the reflected fluxes. The technique consists of the creation of a dynamic component of the surface temperature by using a modulated photothermal effect. A modulated component appears in the signal due to the emitted flux, whereas the reflected flux only contributes to the DC signal. Experimental surface temperature measurements of a sample placed in a furnace have been reported. Although the reflected flux on the sample is much higher than the flux emitted by the sample, no systematic error appears when using surface temperature measurement by the photothermal effect. It has also been shown that this technique can be applied to low temperatures. In fact, measurements as low as 340 K by using a two-color approach and down to 300 K by means of a calibrated approach are reported. Moreover, since the detected dynamic component of the signal is due to the flux emitted by the illuminated region, we obtain very good spatial resolution for the temperature measurement. Furthermore, impulse heating can be created by means of a pulsed laser allowing both high spatial resolution and high temporal resolution for the temperature measurement. The pulsed technique is presently being developed, and should allow surface temperature measurements for moving targets.

Appendix A

For a stationary Gaussian laser beam of power P_0 and emission wavelength λ_0, the temperature distribution[32] at the surface of the sample can be written in the form

$$\Delta T_0(r) = \frac{P}{2\sqrt{\pi}kw}\exp\left[\frac{-r^2}{2w^2}\right] I_0\left[\frac{r^2}{2w^2}\right] \tag{A1}$$

where $P = \alpha_{\lambda_0} P_0$, P is the absorbed laser power, α_{λ_0} is the absorptivity of the target at the laser wavelength, w the beam waist on the surface, and k the thermal conductivity of the sample. I_0 is the zeroth-order modified Bessel Function.

When the beam is modulated at frequency f, the solution $\Delta T_0(r,f)$, for the first harmonic temperature distribution[33,34] is

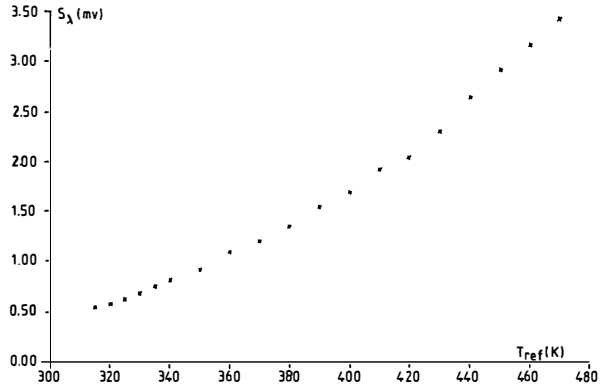

Fig. 9. Photothermal signal S_λ vs reference temperature T_{ref} for a stainless steel sample, with the following experimental parameters: $P_0 = 2$ W, $f = 35$ Hz, bandwidth $\Delta\lambda = 2.2$ μm, and $\epsilon' = 0.4$.

$$\Delta T_1(r,f) = \frac{P\kappa_{\lambda_0}}{\pi^2 k}\int_0^\infty \frac{\exp\left[\frac{-x^4}{4}\right] J_0\left[\frac{xr}{w}\right] x}{(\kappa_{\lambda_0} w + \zeta)\zeta}\,dx, \tag{A2}$$

where

$$\zeta^2 = \frac{2\pi j f w^2}{D} + x^2,$$

κ_{λ_0} is the absorption coefficient, D the thermal diffusivity of the sample, and J_0 is the zeroth-order Bessel Function.

Appendix B

In this section, we show that the main features of ΔT_1 can be described in a straightforward way. We assume that the sample is a semi-infinite graybody in black surroundings at temperature T_a and is irradiated by a uniform time dependent heat source. Heat convection exchanges are described by a heat transfer coefficient h.

Without perturbation, the stationary field temperature is defined by a differential equation and two boundary conditions. For brevity we only specify the flux continuity condition across the interface which contains all the information about the heat transfer at the interface

$$\frac{\partial^2 T_0}{\partial x^2} = 0$$

$$-k\left(\frac{\partial T_0}{\partial x}\right) = \epsilon\sigma(T_0^4 - T_a^4) + h(T_0 - T_a)$$

where ϵ is the isotropic emissivity of a graybody, k the thermal conductivity, and σ the Stefan-Boltzmann constant. The temperature modification due to a time dependent noncontact heat source provides a variation that we denote $T - T_0$ and defined by

$$\frac{\partial^2 (T - T_0)}{\partial x^2} = D\frac{\partial (T - T_0)}{\partial t}$$

$$-k\left(\frac{\partial (T - T_0)}{\partial x}\right) = -P + 4\epsilon\sigma T^3 (T - T_0) + h(T - T_0),$$

where P is the time dependent absorbed flux and D the thermal diffusivity. An additional initial condition should be used for the time dependent case. In the last equation, the two last terms are negligible compared to the absorbed flux P. An analysis of the simplified system shows that two dimensionless numbers appear. From the continuity condition, we introduce a characteristic temperature PL/k whereas from the differential equation, we introduce the Fourier number F

$$T^+ = (T - T_0)/[PL/k] \quad \text{and} \quad F = Dt/L^2,$$

where L is a characteristic length of the temperature field. Note that no characteristic length appears in the geometry of the problem since we deal with a semi-infinite geometry uniformly irradiated. The only characteristic length can be deduced through the Fourier number using the only characteristic time $1/\omega$.

$$L = \sqrt{\frac{D}{\omega}}.$$

Thus, the characteristic temperature PL/k can be put in the form

$$\frac{P}{k}\sqrt{\frac{D}{\omega}}.$$

Since the physical parameters do not appear in the dimensionless differential system, this result gives the dependence of T on k, D, P, and ω which can be deduced from an asymptotic expansion of (A2).

References

1. Y. S. Touloukian and D. P. De. Witt, "Thermophysical Properties of Matter," **9,** IFI (Plenum, New York, 1970).
2. E. M. Sparrow and R. D. Cess, *Radiation Heat Transfer* (McGraw-Hill, New York, 1978).
3. K. H. Berry, "Who Needs Measurements of Emissivity?," Proc. Soc. Photo-Opt. Instrum. Eng. **234,** 56– (1980).
4. G. D. Nutter, "Radiation Thermometry," Mech. Eng. **12,** 12–15 (1972).
5. A. Janest and B. Passier, "Procédé et Dispositif Pyrométrique pour Déterminer à Distance par Voie Optique la Température et ou L'émissivité d'un Corps ou Milieu Quelconque," Brevet d'Invention FR 2572523 (2 May 1986).
6. J. L. Gardner, "Computer Modelling of a Multiwavelength Pyrometer for Measuring True Surface Temperature," High Temp.–High. Pressures **12,** 699–705 (1980).
7. J. L. Gardner, T. P. Jones, and M. R. Davies, "A Six Wavelength Radiation Pyrometer," High Temp.-High. Pressures **13,** 459–466 (1981).
8. P. B. Coates, "Multiwavelength Pyrometry," Metrologia **17,** 103–109 (1981).
9. G. Ruffino, "Increasing Precision in Two-Colour Pyrometry," Temperature Measurement, Inst. Conf. Ser. N^{0}26-264-72, (1975).
10. D. P. De. Witt and H. Kunz, "Theory and Technique for Surface Temperature Determinations by Measuring the Radiance Temperatures and the Absorptance Ratio for Two Wavelengths," *Temperature: Its Measurement and Control in Science and Industry*, H. H. Plumb, Ed. (Instrument Society of America, Pittsburgh, 1972) Vol. **4,** Part 1, pp. 596–610.
11. M. Charpenel and J. Wilhelm, "Pyrométrie Infrarouge pour la Mesure de Température d'Aubes de Turbines," *Symposium AGARD, Echanges Thermiques et Refroidissement dans les Moteurs à Turbines*, Norvège, 6–10 May (1985).
12. J. E. Roney, "Steel Surface Temperature Measurement in Industrial Furnaces by Compensation for Reflected Radiation Errors," *Temperature: Its Measurement and Control in Science and Industry*, J. F. Schooley, Ed. (Instrument Society of America, Pittsburgh, 1982) Vol. **5,** p. 485.
13. P. Cielo, *Optical Techniques for Industrial Inspection* (Industrial Materials Research Institute National Research Council Canada, Academic, New York, 1987).
14. T. Land, "Practical Aspect of Radiation Pyrometry," Trans. Soc. Instr. Techn. March, (1959).
15. D. Ramelot, J. M. Ludovicy, C. Stolz, and J. P. Fischbach, "Capteurs Industriels Pour Applications aux Basses Températures," Rev. Gén. Therm. **23,** 517–524 (1988).
16. J. J. Greffet and T. Loarer, "Pyrométrie par effet Photothermique Modulé ou Impulsionnel," MESUCORA 1988, 14–18 November, 10th International Exposition, Paris, (1988).
17. R. D. Cowan, "Proposed Method of Measuring Thermal Diffusivity at High Temperatures," J. Appl. Phys. **32,** 1363–1370 (1961).
18. P. E. Nordal and S. O. Kanstad, "New Development in Photothermal Radiometry," Infrared Phys. **25,** 295–304 (1985).
19. O. Berthet, J. J. Greffet, and Y. Denayrolles," Procédé de Mesure de la Température d'un Corps Par Détection Optique et Échauffement Modulé." Brevet Français d'Invention N^0:8611542 du (8 août 1986).
20. O. Berthet, J. J. Greffet, "Pyrometry by Photothermal Effect," *Proc. of the Eight International Heat Transfer Conference*, San Francisco, (1986), pp. 561–564.
21. O. Berthet, "Effet Photothermique Appliqué à la Pyrometrie Optique," Thèse de Doctorat, Ecole Centrale, Paris, (1987).
22. A. Rosencwaig and A. Gersho, "Theory of the Photoacoustic Effect with Solids," J. Appl. Phys. **47,** 66–69 (1976).
23. W. L. Wolfe and G. J. Zissis, *The Infrared Handbook* (IRIA, Environmental Research Institute of Michigan, Ann Arbor, MI, 1978).
24. R. Barber, "Non-Contact Temperature Measurements of Metal Surfaces in the Open," *Proc. ISA-78, Conf, Advance in Instrumentation* (The Instrument Society of America, Research Triangle Park, N.C., 1978), p. 142.
25. A. Soufiani, "Etudes Théoriques et Expérimentales des Transferts Couplés par Convection Laminaire ou Turbulente et Rayonnement dans un Milieu Gazeux à Température élevée," Thèse de Doctorat d'Etat N^{0}3384, Paris-Sud Orsay (1987).
26. H. J. Kostkowski and R. D. Lee, "Theory and Methods of Optical Pyrometry," *Temperature: Its Measurement and Control in Science and Industry*, F. C. Brickwedde, Ed., American Institute of Physics (Reinhold, New York, 1962) Vol. **3,** Part 1, pp. 449–481.
27. J. L. Gardner, "Effective Wavelength for Multicolor/Pyrometry," Appl. Opt. **19,** 3088–3091 (1980).
28. J. Bezemer, "Spectral Sensitivity Corrections for Optical Standard Pyrometers," Metrologia **10,** 47–52 (1974).
29. P. B. Coates, "Wavelength Specification in Optical and Photoelectric Pyrometry," Metrologia **13,** 1–5 (1977).
30. J. W. Hahn and C. Rhee," Reference Wavelength Method for Two-Color Pyrometer," Appl. Opt. **26,** 5276–5279 (1987).
31. J. W. Hahn and C. Rhee, "Calculation of Temperature Error in Two-Color Pyrometer Designed with the Reference Wavelength Method," Appl. Opt. **27,** 1916–1918 (1988).
32. M. Lax, "Temperature Rise Induced by a Laser Beam," J. Appl. Phys. **48,** 3919–3924 (1977).
33. W. B. Jackson, N. M. Amer, A. C. Boccara, and D. Fournier, "Photothermal Deflection Spectroscopy and Detection," Appl. Opt. **20,** 1333–1344 (1981).
34. H. C. Chow, "Theory of Three Dimensional Photoacoustic Effect with Solids," J. Appl. Phys. **51,** 4053–4058 (1980).